PhD Defense

UNDERWATER ROBOTS FOR KARST AND MARINE EXPLORATION: A STUDY OF REDUNDANT AUVs

Tho DANG

EXPLORE team, LIRMM, Montpellier University

May 25, 2021

Projet cofinancé par le Fonds Social Européen

Juries

René Zapata	Professeur	LIRMM Montpellier	Président du jury
Lionel Lapierre	MCF, HDR	LIRMM Montpellier	Directeur de thèse
Luc Jaulin	Professeur	Lab-STICC Bretagne	Rapporteur
Vincent Hugel	Professeur	COSMER Toulon	Rapporteur
Antonio Pascoal	Professeur	IST-ID Portugal	Examinateur
Massimo Caccia	Professeur	CNR ISSIA Italy	Examinateur
Olivier Parodi	IR	Naval Group	Examinateur
Benoit Ropars	IR	Reeds	Examinateur

Outline

Outline

Introduction - Ocean and Karst exploration

Open-environment

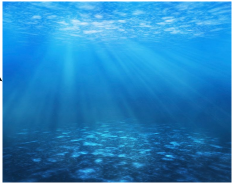

(a) Ocean

Confined-environment

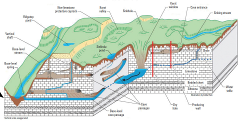

(b) Karst

Ocean and Karst [1]

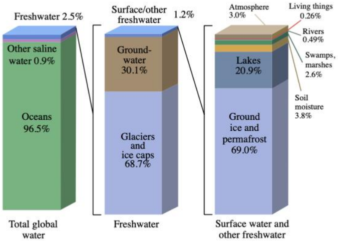

Figure 1: Where is Water of Earth? [2]

1. Resource of Earth water
2. Water resource management

[1] Taylor2008hydrogeologic

[2] Gleick1993

Karst exploration - Challenges

Challenges for karst exploration are as follows:

1. Umbilical cable management
2. Navigation and Mapping
3. Guidance and Control
4. Robustness
5. Reactivity and adaptable autonomy
6. Redundancy management

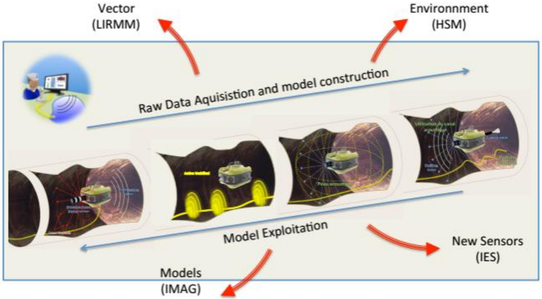

Figure 2: Karst exploration concepts (ALEYIN project): French institutes: LIRMM, HSM, IMAG, IES

Objectives of the thesis

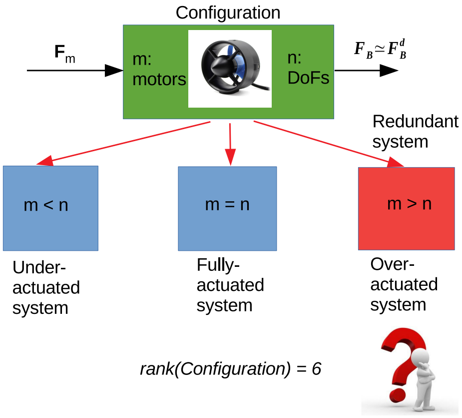

Figure 3: Configuration of a robot

The thesis focuses on *Configuration* in Actuation System of a robot:

1. Static configuration (*thrusters are fixed*):
   a. Propose performance indices.
   b. Find a Pareto optimal solution.
   c. Simulate and carry out experiments
2. Reconfigurable and dynamic configuration (*thruster's position/direction can be dynamically modified*):
   a. Build a reconfigurable robot - Umbrella Robot (UmRobot).
   b. Propose dynamic configuration problem.
   c. Simulate and carry out experiments on UmRobot.

Outline

Background - Kinematic and dynamic models

Kinematic model:

1. Euler formalism:

$$\dot{\eta} = \mathbf{J}(\eta)\nu \tag{1}$$

   where **J** is a matrix including rotation and transformation sub-matrices.

2. Quaternion formalism: $\begin{bmatrix} \dot{\eta}_{1Q} \\ \dot{\mathbf{Q}} \end{bmatrix} = \begin{bmatrix} \mathbf{Q} \odot \begin{bmatrix} 0 \\ \nu_1 \end{bmatrix} \odot \mathbf{Q}^* \\ \frac{1}{2}\mathbf{Q} \odot \mathbf{W} \end{bmatrix}$

Dynamic model:

$$\mathbf{M}\dot{\nu} = \mathbf{F}_B + \mathbf{F}_{wind} + \mathbf{F}_{wave} - \mathbf{C}(\nu)\nu - \mathbf{D}(\nu)\nu - \mathbf{g}(\eta) \tag{2}$$

where **M** is rigid-body mass matrix (including added mass), **C** is Corriolis-Centripetal matrix, **D** is damping matrix, **g** is buoyancy force. $\mathbf{F}_{wind}$ and $\mathbf{F}_{wave}$ are environmental forces/moments (wind and wave).

Background - Mono-objective and Multi-objective optimizations

Mono-objective:

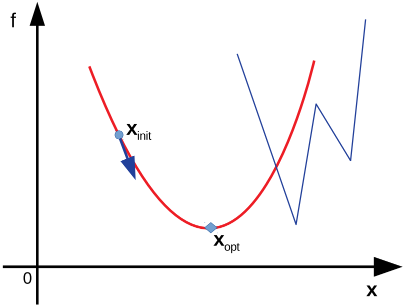

Figure 4: Mono-objective optimization

Multi-objective:

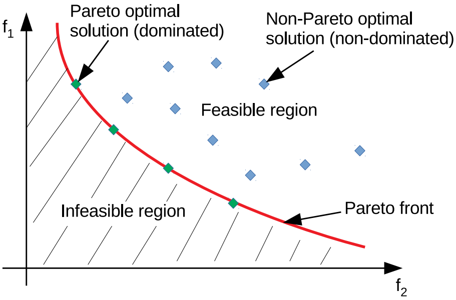

Figure 5: Pareto optimal point and Pareto front

Outline

Robot's configuration and configuration matrix

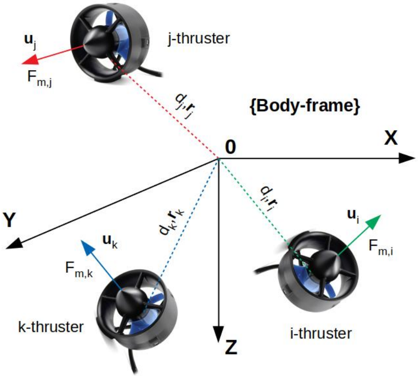

Figure 6: Actuators configuration model

The configuration matrix **A** is described:

$$\mathbf{A} = \begin{pmatrix} \mathbf{A}_1 \\ \mathbf{A}_2 \end{pmatrix} \quad (3)$$

thrusters are fixed

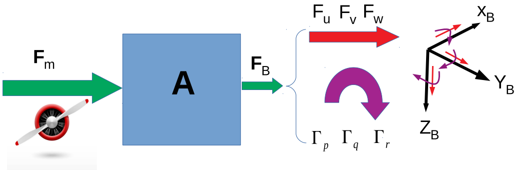

Figure 7: Configuration matrix

Performance indices

1. Manipulability index
2. Energetic index
3. Workspace index
4. Reactive index
5. Robustness index

Manipulability index

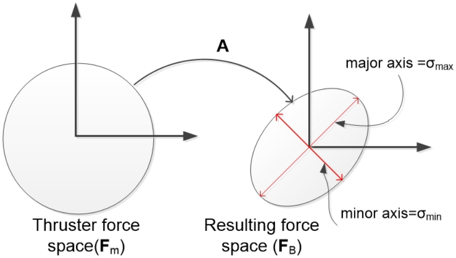

Figure 8: Manipulability ellipsoid with mapping

Manipulability index is defined as:

$$I_m = Cond(\mathbf{A}) = \frac{\sigma_{max}}{\sigma_{min}} \quad (4)$$

where σ_{max} and σ_{min} are the maximum and minimum singular value of configuration matrix, **A**, respectively.

Isotropy: the robot can act equally in all directions

Energetic index

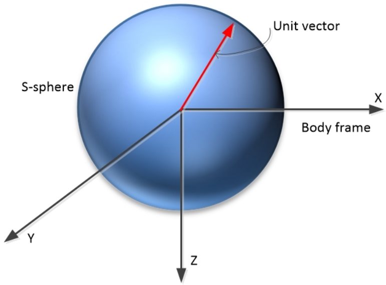

Figure 9: The unit desired vector in 3D sphere

Energetic index is defined as:

$$I_e = \frac{1}{S}\int_S (w_{ef}p_{Ef} + w_{e\tau}p_{E\Gamma})dS \quad (5)$$

where w_{ef} and $w_{e\tau}$ are weighting scalars.

$$\begin{cases} p_{Ef} = \left\|\mathbf{A}^+\binom{\mathbf{u}_s}{\mathbf{0}}\right\|, & \text{force sphere} \\ p_{E\Gamma} = \left\|\mathbf{A}^+\binom{\mathbf{0}}{\mathbf{u}_s}\right\|, & \text{torque sphere.} \end{cases}$$

$\mathbf{u}_s$ is a unit vector in 3D-sphere.

Workspace index

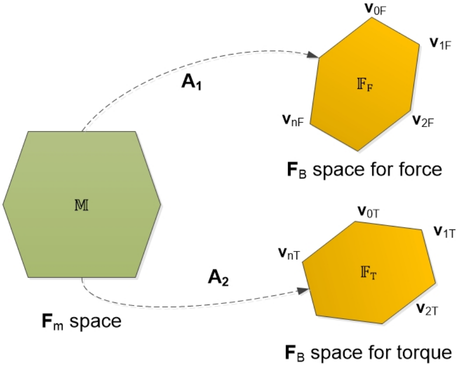

Figure 10: Space Mapping

Workspace index is defined as:

$$I_w = \omega_{wf} Vol(\mathbb{F}_F) + \omega_{wT} Vol(\mathbb{F}_T) \quad (6)$$

where *Vol* is the volume measure of a space ($\mathbb{F}_F$-force space, $\mathbb{F}_T$-torque space), ω_{wf} and ω_{wT} are weighting coefficients.

Reactive index

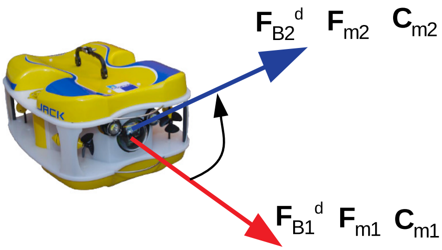

Figure 11: Robot changes its motion direction

How fast the robot can change the direction of its actuation force. Reactive index is defined as:

$$I_{re} = \|\mathbf{A}^{+}\| \tag{7}$$

Robustness index

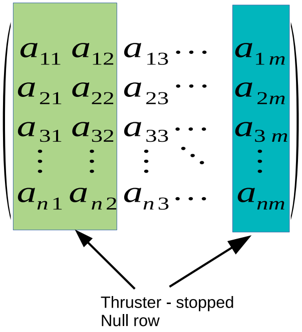

Figure 12: One or more thrusters - be stopped

Robustness index is defined as:

$$I_{ro} = rank(\mathbf{A}|_{\leq m-6}) = 6 \qquad (8)$$

where $\mathbf{A}|_{\leq m-6}$ is the $\mathbf{A}$ matrix with the maximum number of columns being zero is $(m-6)$.

Problem formulation

Static configuration problem is written as:

$$\min_{\mathbf{A}} \mathbf{V}(\mathbf{A}) = \min_{\mathbf{A}} [I_m \; I_e \; \frac{1}{I_w} \; I_{re}]^T \quad (9)$$
$$s.t \quad \mathbf{A} \in \mathbb{A}$$

where $\mathbf{A}$ is matrix variable. $\mathbb{A}$ is the constraint set including constraints of positions and orientations of thrusters, and robustness index.

The problem is rewritten clearly:

$$\min_{\mathbf{A}(\mathbf{u},\boldsymbol{\tau})} \mathbf{V}(\mathbf{A}) = \min_{\mathbf{A}} [I_m, I_e, \frac{1}{I_w}, I_{re}]^T \quad (10)$$

$$\begin{aligned} s.t \quad & \|\mathbf{u}_i\| = 1, i = 1, 2, ...m \\ & \|\boldsymbol{\tau}_i\| \leq 1, i = 1, 2, ...m \\ & \boldsymbol{\tau}_i^T \mathbf{u}_i = 0, i = 1, 2, ...m \\ & I_{ro} = rank(\mathbf{A}|_{\leq m-6}) = 6 \end{aligned}$$

Ball robot and Cube robot - Design

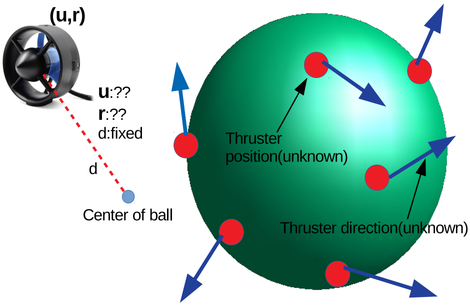

Figure 13: Ball robot concept

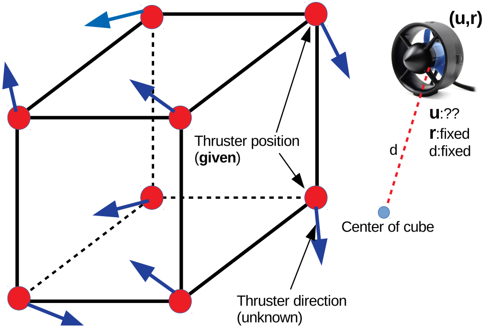

Figure 14: Cube robot concept

Solution

Process of searching Pareto optimal solution

1. Phase 1: Find one Pareto solution of configuration matrix with goal attainment method.
2. Phase 2: Check robustness index of the chosen solution in phase 1.

Design a robot with $m = 8$ thrusters and $n = 6$ DoFs ($\sigma_{max} = \sqrt{2\frac{m}{n}}$).

Index	Optimal formula and condition	Desired Value
I_m	$\sigma_{max} = \sigma_{min}$	1
I_e	$2 \lVert \mathbf{A}^+ \rVert$	1.2248
I_w	$I_w = I_{wF} + I_{wT}$	303.0303
I_{re}	$\frac{1}{\sigma_{max}}$	0.6124

Table 1: Desired values of indices ($m = 8$ thrusters)

Simulation - General case

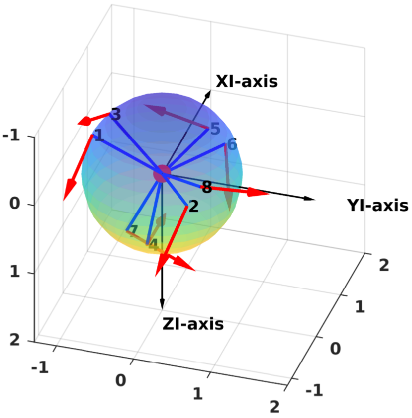

Figure 15: Robot design (Ball robot - general case) with 8 thrusters

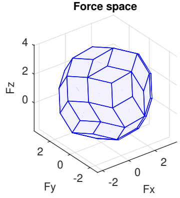

(a) Force space attainability

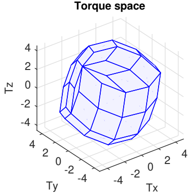

(b) Torque space attainability

Figure 16: Force and Torque attainable spaces

Simulations - given position case

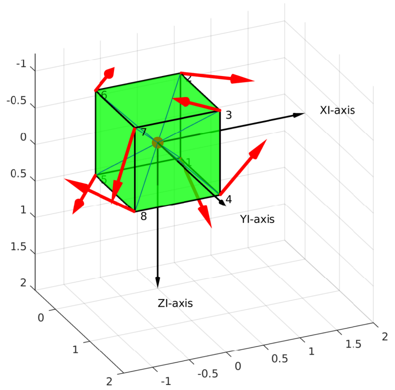

Figure 17: Robot design (Cube robot - given position case)

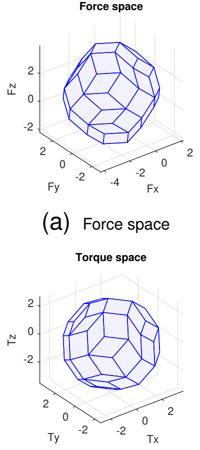

(a) Force space

(b) Torque space

Figure 18: Force and Torque spaces

Simulation - A comparison on Cube's robot

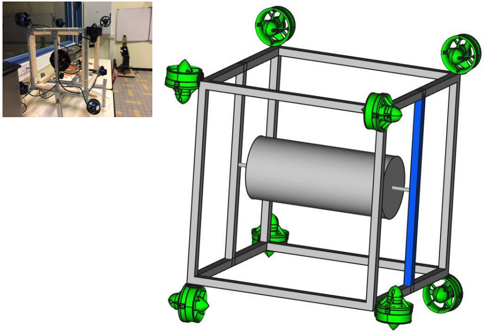

(a) Cube robot in $\mathbf{C}^1$ configuration

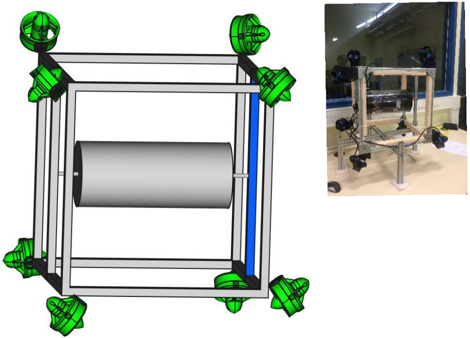

(b) Cube robot in $\mathbf{C}^2$ configuration

Figure 19: Cube robot in two configurations $\mathbf{C}^1$ and $\mathbf{C}^2$

Simulations- A comparison

No.	Indices	$\mathbf{C}^1$	$\mathbf{C}^2$
1	I_m	7.12	2.5592
2	I_e	3.32	2.09
3	I_w	6511536.45	10919428.13
4	I_{re}	4.05	1.5622
5	I_{ro} [1]	0	2

Table 2: Performance indices of two configurations

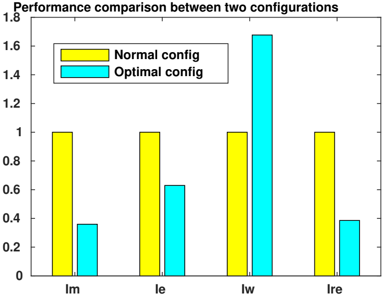

Figure 20: Comparison between two configurations

[1] the maximum number of thrusters which can be failed to make sure that $rank(\mathbf{A}) = 6$

Simulations - A comparison

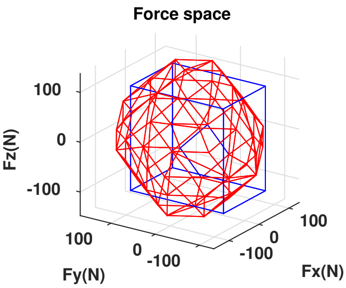

(a) $\mathbf{c}^1$ (blue), $\mathbf{c}^2$ (red)

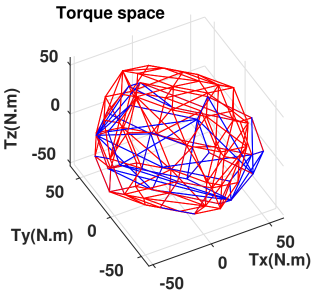

(b) $\mathbf{c}^1$ (blue), $\mathbf{c}^2$ (red)

Figure 21: Attainable spaces of two configurations

Simulations - A comparison - Attainability about X-axis

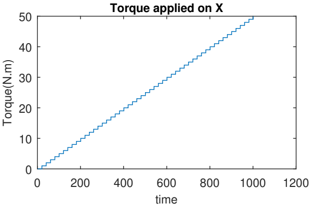

Figure 22: Applied torque about X-axis

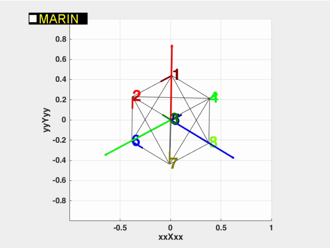

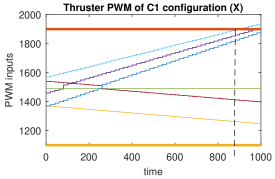

(a) PWM inputs of $\mathbf{c}^1$

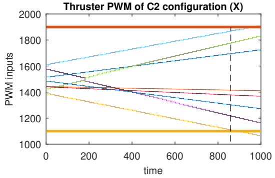

(b) PWM inputs of $\mathbf{c}^2$

Figure 23: The simulation of cube rotation about X-axis for $\mathbf{c}^1$ and $\mathbf{c}^2$

Simulations - A comparison - Attainability about Y and Z-axis

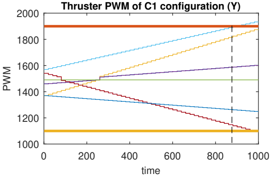

(a) PWM inputs of C1

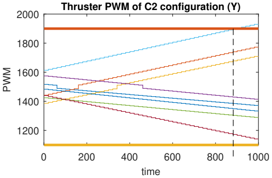

(b) PWM inputs of C2

Figure 24: The simulation of cube rotation about Y-axis for $\mathbf{C}^1$ and $\mathbf{C}^2$

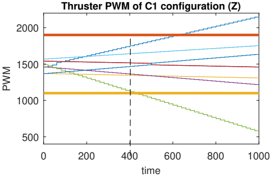

(a) PWM inputs of C1

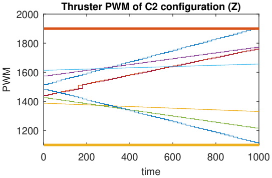

(b) PWM inputs of C2

Figure 25: The simulation of cube rotation about Z-axis for $\mathbf{C}^1$ and $\mathbf{C}^2$

Experimental results - Cube description

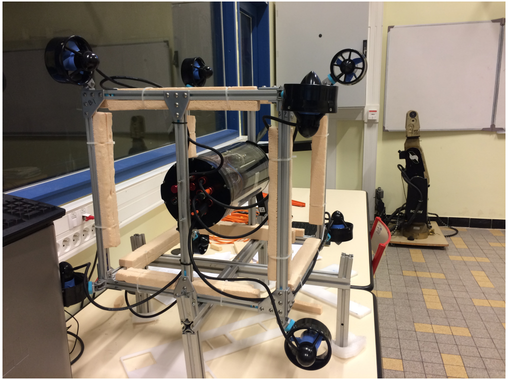

Figure 26: $\mathbf{C}^1$ configuration

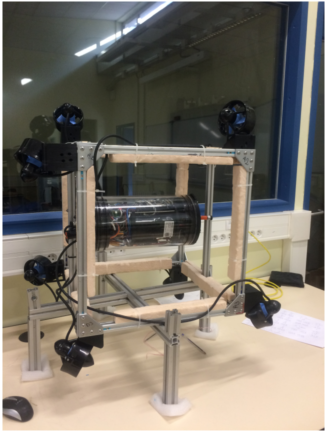

Figure 27: $\mathbf{C}^2$ configuration

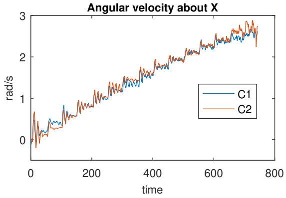

(a) Angular velocities - X axis

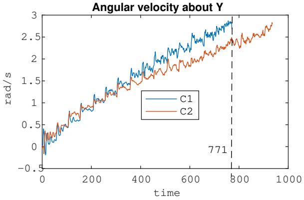

(b) Angular velocities - Y axis

Figure 28: About X and Y-axis for $\mathbf{C}^1$ and $\mathbf{C}^2$

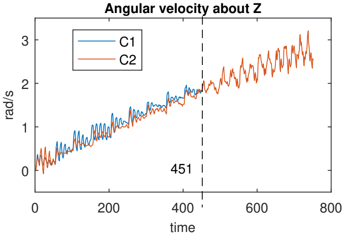

Figure 29: About Z-axis for $\mathbf{C}^1$ and $\mathbf{C}^2$

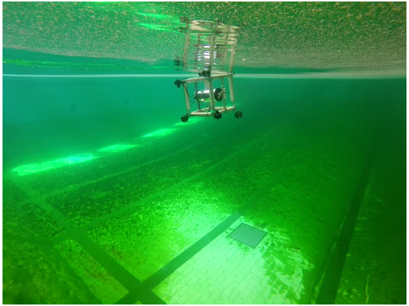

Experimental results - Energetic validation

The energetic-like criterion is computed as:

$$\mathbf{E} = \sum_{i=1}^{m} \int_{t=0}^{T} |PWM^i(t) - 1500| dt \qquad (11)$$

No.	Rotation	$\mathbf{E}_{\mathbf{C}^1}$	$\mathbf{E}_{\mathbf{C}^2}$	Percentage
1	*p*	7.2303e+04	6.9603e+04	3.73 %
2	*q*	7.5480e+04	1.0590e+05	see Table 4
3	*r*	3.1637e+04	7.4350e+04	see Table 4

Table 3: Energy consumption of two configurations

No.	Rotation	$\mathbf{E}_{\mathbf{C}^1}$	$\mathbf{E}_{\mathbf{C}^2}$	Percentage
1	*q*	7.5480e+04	7.2715e+04	3.66 %
2	*r*	3.1637e+04	3.3312e+04	-5.03 %

Table 4: Energy consumption of two configurations with the same time duration

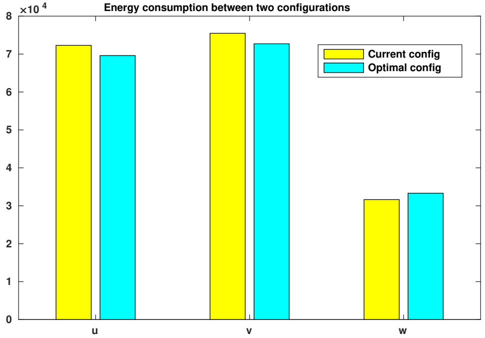

Figure 30: Energetic-like consumption between two configurations

Experimental results - Robustness and reactive validations

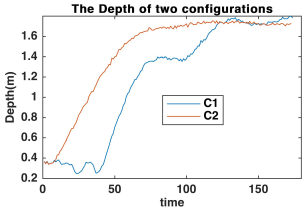

Figure 31: Depth control for **C**[1] and **C**[2] with three motors stopped

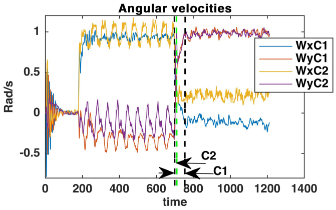

Figure 32: Angular velocity evaluation for **C**[1] and **C**[2]: diving, rotating X-axis, and rotating Y-axis

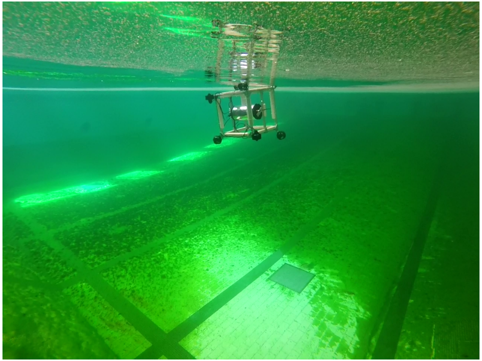

Outline

Reconfigurable robot - A glance

Figure 33: Tortuga ROV - SubSea Tech

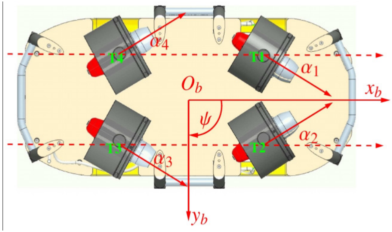

Figure 34: Reconfigurable principle of Tortuga

Reconfigurable robot Design

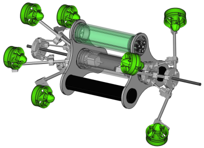

(a) Umbrella robot in *open-forward*

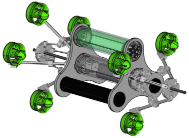

(b) Umbrella robot in *close*

Figure 35: The 3D model of UmRobot

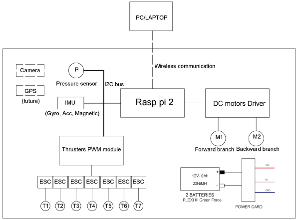

Figure 36: The principle diagram of UmRobot

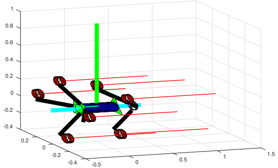

Figure 37: Umbrella robot like Torpedo

The robot includes:

1. Two branches (front and rear) controlled by two DC motors
2. Rasp pi 2
3. Pressure sensor
4. IMU
5. 7 thrusters

One robot - different configurations

Prototype

Figure 38: A prototype of Umbrella Robot

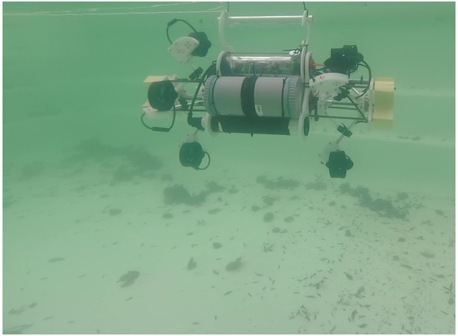

Figure 39: A prototype of Umbrella Robot in water

Simulations-Manipulability index

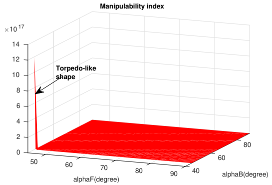

Figure 40: Manipulability index of Umbrella robot

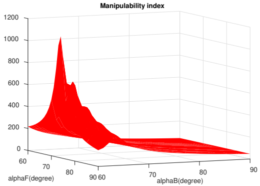

Figure 41: Manipulability index [60° − 90°]

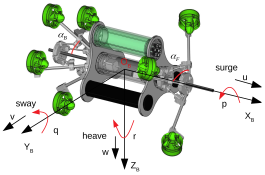

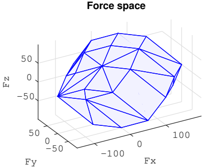

(a) Attainable force space

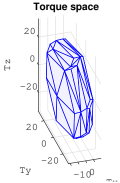

(b) Attainable torque space

Figure 42: Attainable space if $\alpha_F = \alpha_B = 90^0$

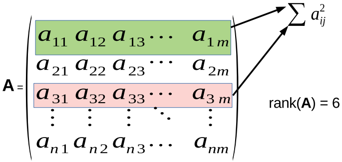

Figure 43: Acting ability

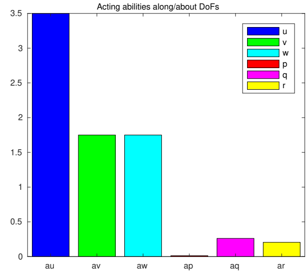

Figure 44: with $\alpha_F = \alpha_B = 90^0$

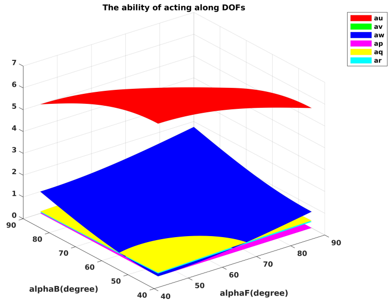

Figure 45: with varying α_F and α_B

Acting ability - Optimization problem

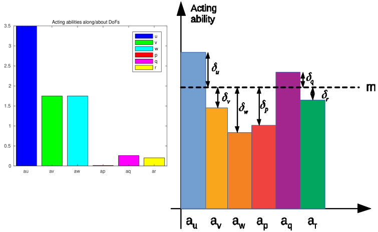

Figure 46: Acting ability along each DOFs and deviations

No.	Variable	Optimal value
1	α_F	90°
2	α_B	45°
3	d	$0.5(m)$
4	d_e	$0.2(m)$
5	d_t	$0.2(m)$
6	d_c	$0.0914(m)$
7	d_b	$0.15(m)$
8	az_i, el_i(rad)	$\begin{pmatrix} az_1 = 0.6106 & el_1 = 2.2317 \\ az_2 = 1.7060 & el_2 = 0.4642 \\ az_3 = -0.6106 & el_3 = -0.9099 \\ az_4 = -0.3754 & el_4 = 2.6030 \\ az_5 = 0.1261 & el_5 = -2.5692 \\ az_6 = 2.9525 & el_6 = -1.9817 \\ az_7 = 3.0155 & el_7 = 0.5724 \end{pmatrix}$

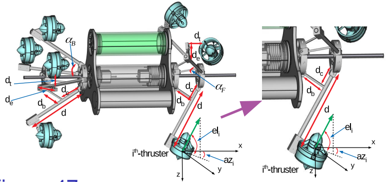

Figure 47: variables in configuration optimization problem

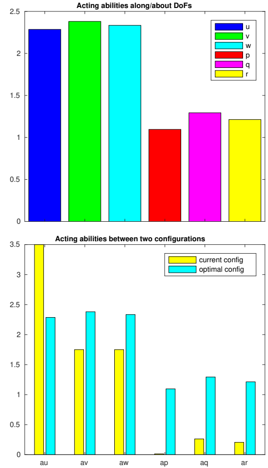

Figure 48: Optimal acting of Umbrella robot and the comparison with current configuration

Experiment results - Yaw control

Figure 49: Umbrella Robot at the swimming pool

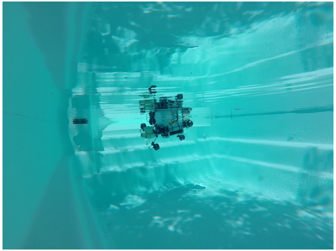

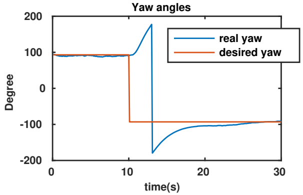

(a) Yaw angles

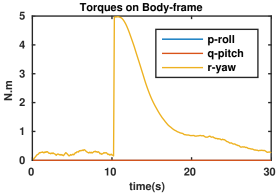

(b) Applied torques

Figure 50: Yaw control

Experiment results - Depth control

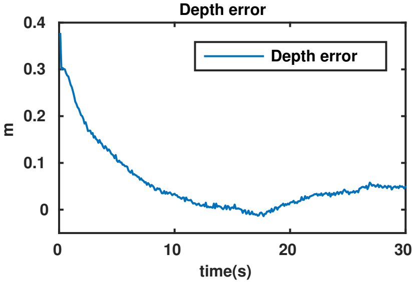

Figure 51: Depth error

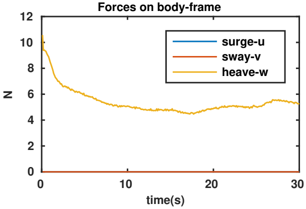

Figure 52: Applied forces

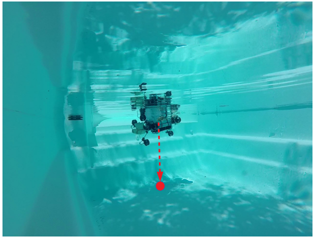

Figure 53: Mission descriptions

The robot has to open the umbrella.

Experiment results - Surge, pitch, yaw control

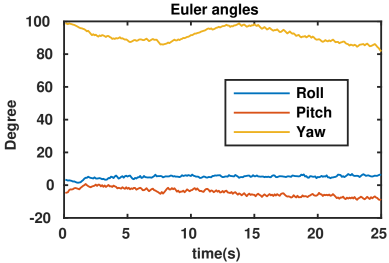

Figure 54: Euler angles

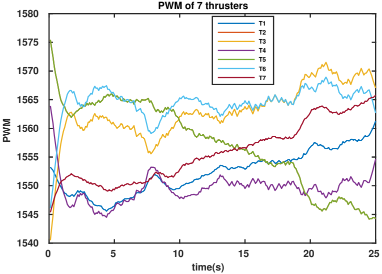

Figure 55: PWM of thrusters

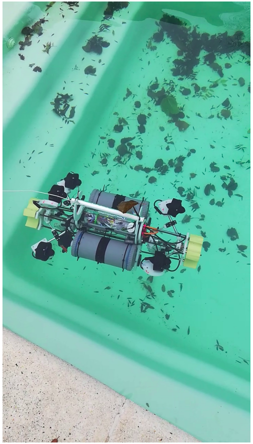

Experiment results - Integrated mission

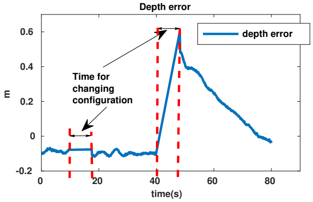

(a) Depth error

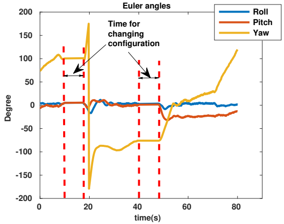

(b) Euler angles

Figure 56: Integrated Mission of UmRobot

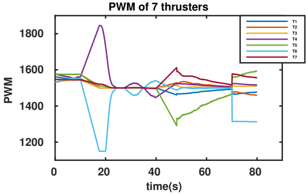

Figure 57: PWM of thrusters

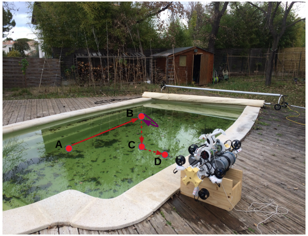

Figure 58: Mission descriptions

The robot surges forward, turns back, dives to desired depth, and finally sways.

A Toolbox

A toolbox for validating performance indices and acting abilities of a robot

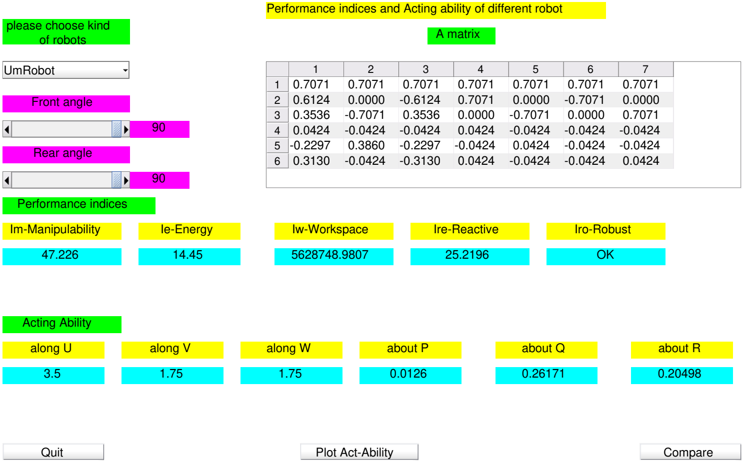

	1	2	3	4	5	6	7
1	0.7071	0.7071	0.7071	0.7071	0.7071	0.7071	0.7071
2	0.6124	0.0000	-0.6124	0.7071	0.0000	-0.7071	0.0000
3	0.3536	-0.7071	0.3536	0.0000	-0.7071	0.0000	0.7071
4	0.0424	-0.0424	-0.0424	0.0424	-0.0424	-0.0424	-0.0424
5	-0.2297	0.3860	-0.2297	-0.0424	0.0424	-0.0424	-0.0424
6	0.3130	-0.0424	-0.3130	0.0424	-0.0424	-0.0424	0.0424

Figure 59: Toolbox for configuration evaluation: main page

Outline

Dynamic configuration problem

With capacity of varying configurations, how can we choose a proper one? A-SQP approach

$$\min_{\alpha_F, \alpha_B, \mathbf{F}_m} J = \|\mathbf{F}_m\|^2 \tag{12a}$$

$$s.t \quad 45^0 \leq \alpha_F, \alpha_B \leq 90^0 \tag{12b}$$

$$\mathbf{F}_m \in \mathbb{F} \tag{12c}$$

$$\mathbf{F}_B^d - \mathbf{A}(\alpha_F, \alpha_B)\mathbf{F}_m = 0 \tag{12d}$$

where $\mathbf{F}_B^d$ is desired control vector (from the controller), $\mathbb{F}$ is a feasible set of thrusters forces. The constraint (12b) is mechanical limitations of the Umbrella robot.

Simulations

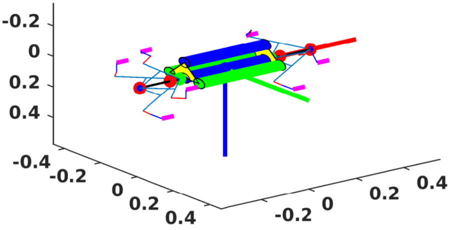

Figure 60: Simulated robot

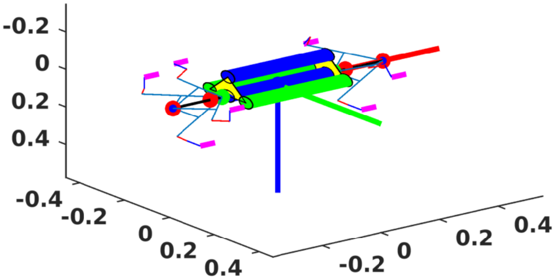

Simulations - Given desired control vector

Given desired control vector $\mathbf{F}_B^d$

No	desired control vector
1	$\mathbf{F}_B^d = [10 \quad 0 \quad 0 \quad 0 \quad 0 \quad 0]^T$
2	$\mathbf{F}_B^d = [10 \quad 10 \quad 0 \quad 0 \quad 0 \quad 0]^T$
3	$\mathbf{F}_B^d = [0 \quad 0 \quad 10 \quad 0 \quad 0 \quad 0]^T$

1. Configuration with $\alpha_F = \alpha_B = 90^0$
2. Configuration with $\alpha_F = 60^0$ and $\alpha_B = 70^0$
3. Optimal configuration (statically)
4. Dynamic configuration

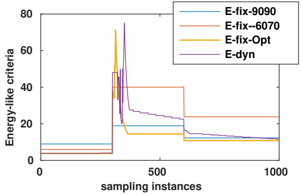

Figure 61: Evolution of energy-like criterion with different cases

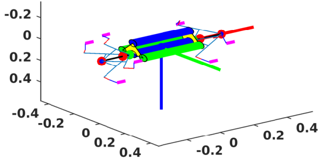

Simulations - Path following problem

The path is parameterized as:

$$x = 60\cos(0.2618s) \qquad (13)$$
$$y = 60\sin(0.2618s) \qquad (14)$$
$$z = \sin(0.2618s) + 5 \qquad (15)$$

where s is a path parameter.

Path following problem with:

1. Configuration with $\alpha_F = \alpha_B = 70^0$
2. Configuration with $\alpha_F = \alpha_B = 90^0$
3. Dynamic configuration.

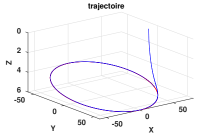

(a) trajectory of Robot in fixed cases

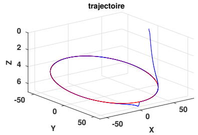

(b) trajectory of Robot in dynamic case

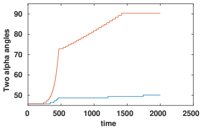

(c) evolution of two angles

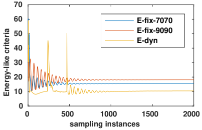

(d) Energy-like criteria for Path following problem

Figure 62: Path following for ellipse with different configurations

Simulations-Observation problem (station-keeping)

Simulations with observation mission: $x = 0$, $y = 0$, $z = 1(m)$ and $p = q = r = 1(rad/s)$

1. Fixed configuration ($\alpha_F = \alpha_B = 90^0$)
2. dynamic configuration with interior-point method (Fmincon function)
3. dynamic configuration with A-SQP

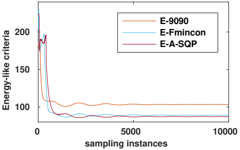

(a) Energy-like criterion evolution

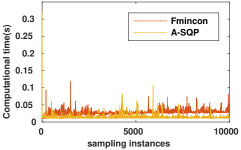

(b) Computational time

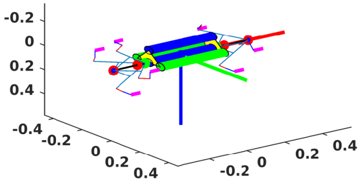

Figure 63: A comparison

Outline

Conclusions and Future works

1. Static configuration design.
2. Reconfigurable robot design.
3. Dynamic configuration problem.
4. Hybrid cube:

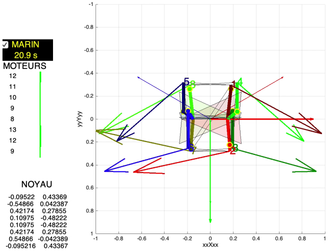

1. Pareto front.
2. Experiments with dynamic configuration problem.
3. Multiparametric programming.
4. Other reconfigurable mechanisms.
5. Efficient control allocation algorithm.
6. Redundancy management

Thank you for your attention